

Quadrupole Moments And Gamma Deformation Of Wobbling Excitations In ^{163}Lu

A. Gorgen*, G.B. Hagemann[†], I. Hamamoto**[†], R. Bengtsson**, R.M. Clark[‡], M. Cromaz[‡], P. Fallon[‡], H. Hubel[§], I.Y. Lee[‡], A.O. Macchiavelli[‡], G. Sletten[†] and D. Ward[‡]

*DAPNIA/SPhN, CEA Saclay, F-91191 Gif-sur-Yvette, France

[†]The Niels Bohr Institute, Blegdamsvej 17, DK-2100 Copenhagen Ø, Denmark

**Department of Mathematical Physics, Lund Institute of Technology, S-22362 Lund, Sweden

[‡]Nuclear Science Division, Lawrence Berkeley National Laboratory, Berkeley, California 94720, USA

[§]HISKP, Universitat Bonn, Nussallee 14-16, D-53115 Bonn, Germany

Abstract. Wobbling is an excitation mode unique to triaxial nuclei. Even though it is a general consequence of triaxiality in nuclei, it has so far only been observed in the odd-mass Lu isotopes around ^{163}Lu . The principal evidence for the wobbling mode is based on the pattern of rotational bands characterized and described by a wobbling phonon number and the decay between different bands belonging to the same family. A new measurement revealed lifetimes of states in an excited wobbling band for the first time and gave access to absolute transition probabilities for both in-band and interband transitions. A general recipe how to derive quadrupole moments for triaxial nuclei from experimental data is discussed. The results show a remarkable similarity of the quadrupole moments for the different bands, further supporting the wobbling scenario. A decrease of the quadrupole moments is observed with increasing spin. This is attributed to an increase in triaxiality with spin, which can at the same time explain the dependence of the interband transitions on spin. Such an increase in triaxiality is qualitatively reproduced by cranking calculations to which the experimental results are compared.

INTRODUCTION

The wobbling mode of excitation in nuclei was first found in ^{163}Lu [1, 2] and is now also established in the neighboring odd-mass Lu isotopes [3, 4, 5]. The phenomenon is uniquely related to nuclei with stable triaxiality. While the triaxial nucleus favors the rotation about the axis with the largest moment of inertia, it can transfer a quantized amount of angular momentum to the the other axes. Such a collective excitation competes with other collective and single-particle excitations, and can be described in terms of a wobbling phonon [6]. In the high-spin limit and neglecting the intrinsic structure, the energies can be separated into the rotation about the principal axis and the wobbling motion: $E(I, n_w) = I(I+1)/(2\mathfrak{I}_x) + \hbar\omega_w(n_w + 1/2)$, where n_w is the wobbling phonon number and ω_w the wobbling frequency, which depends only on the three moments of inertia with respect to the principal axes. As a consequence, the wobbling mode results in a family of rotational bands built on the same intrinsic structure with a phonon-like excitation spectrum between the different bands and enhanced collective $E2$ transitions not only within the bands but also between states with $\Delta I = 1$ and $\Delta n_w = 1$. The strength of the interband transitions $B(E2; n_w \rightarrow n_w - 1)$ should be proportional to n_w/I . The influence of the odd $i_{13/2}$ proton has been studied in particle-rotor calculations [7, 8]. It was shown that it is energetically favorable in the odd Lu cases to keep the unpaired proton aligned and tilt the angular momentum of the core with respect to the axis of the largest moment of inertia to reach states of unfavored signature, thus realizing the wobbling mode in the presence of an unpaired high-j particle. This is schematically illustrated in Fig. 1.

Four triaxial strongly deformed (TSD) bands are observed in ^{163}Lu , the first three of which form a family of wobbling bands with wobbling phonon numbers $n_w = 0, 1, 2$. A partial level scheme of these bands is shown in the left-hand part of Fig. 1. The bands show remarkably similar properties, as is illustrated in the right-hand part of Fig. 1, where the differences in the dynamic moment of inertia and the differences in the alignment of bands TSD2 and 3 are plotted relative to TSD1. The strongest evidence for the wobbling scenario is based on the characteristic properties of the transitions between the bands. Angular correlation and linear polarization measurements [1, 2, 9] have proven

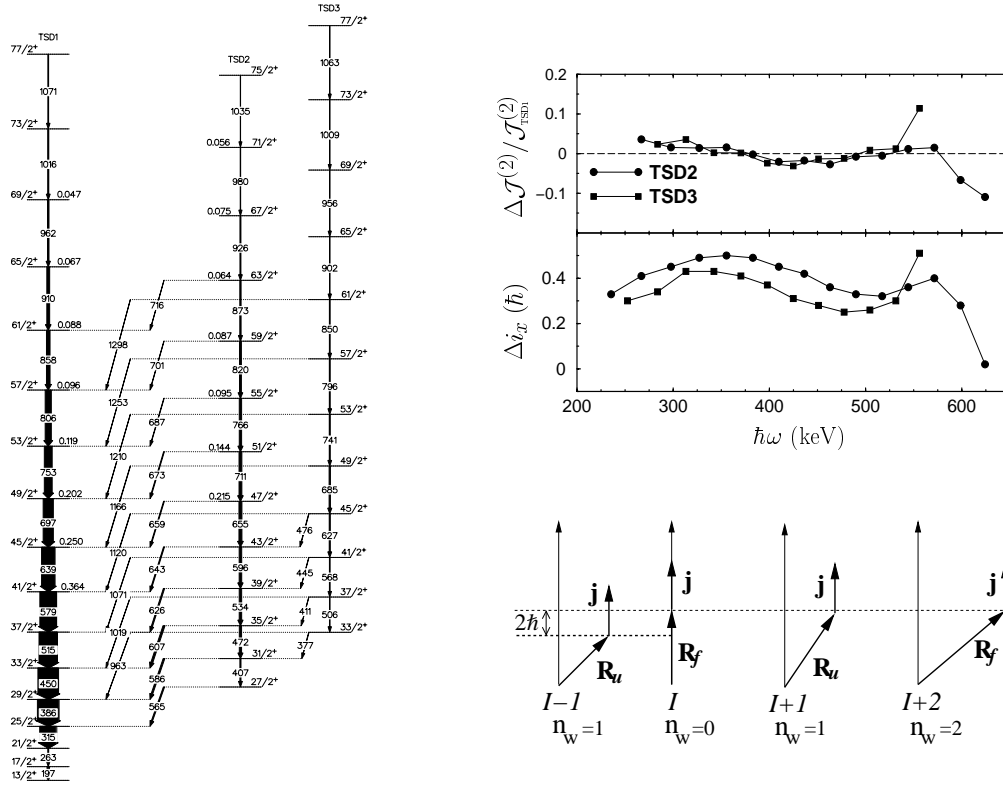


FIGURE 1. *Left:* Level scheme showing the lower part of TSD bands 1, 2, and 3 and the decay between the bands. The full level scheme extending to higher spins and linking the bands to the normal-deformed scheme can be found in Refs. [2, 9]. The lifetimes of states measured in bands TSD1 and 2 are given in picoseconds. *Top right:* Differences between the dynamic moment of inertia and the alignment of bands TSD2 and 3 relative to TSD1 [2]. A rigid reference with $\mathcal{J}_{ref} = 62\hbar^2 \text{ MeV}^{-1}$ was used to extract the alignments. *Bottom right:* schematic coupling scheme of the collective and single-particle angular momenta for different wobbling-phonon numbers.

the (mainly) E2 character of the $\Delta I = 1$ transitions. These strong interband transitions are collective and compete with the enhanced E2 transitions within the strongly deformed bands. Furthermore, the reduced transition probability for the decay from band TSD3 to TSD2, $B(E2; n_w = 2 \rightarrow n_w = 1)$, is about twice as strong as the one for the decay from TSD2 to TSD1, $B(E2; n_w = 1 \rightarrow n_w = 0)$, as expected in the wobbling phonon picture. The ratio $B(E2)_{out}/B(E2)_{in}$ is $\sim 25\%$ for the $n_w = 1 \rightarrow n_w = 0$ transitions, while it is $\sim 50\%$ for the ones with $n_w = 2 \rightarrow n_w = 1$ [2]. Transitions from TSD3 to TSD1 are also observed even though the $\Delta I = 2$, $\Delta n_w = 2$ decay is forbidden in the pure wobbling phonon case. The $B(E2)$ ratios for these transitions are indeed very small ($B(E2)_{out}/B(E2)_{in} \approx 0.02$), and the transitions can only proceed because of their high energy. This decay can be attributed to anharmonicities in the wobbling picture.

Lifetime measurements give access to the shape and can provide a crucial test for the wobbling interpretation. So far only the $B(E2)$ ratios of the interband and in-band transitions have been accessible and been shown to match the expected behavior of wobbling excitations. Absolute $B(E2)$ values can be derived from lifetime measurements. Very similar in-band $B(E2)$ strengths and quadrupole moments are expected for the transitions of the different members of the family of wobbling bands, as they are all built on the same intrinsic structure. Earlier lifetime measurements [10, 11, 12] gave results for band TSD1 only. A new measurement with the Gammasphere spectrometer [13] improved significantly on the previous data and revealed lifetimes for band TSD2 for the first time, so that the wobbling scenario could be tested. Furthermore, the new data provided important insight into the evolution of triaxiality as a function of spin and could simultaneously explain the observed spin dependence of the in-band and interband $B(E2)$ values. Before interpreting the new results it is necessary to discuss the relation between the $B(E2)$ values and the quadrupole moments in a triaxial nucleus, as the formalism to extract quadrupole moments that is usually used for nuclei with axial symmetry is not valid for triaxial nuclei.

SHAPE PARAMETERS AND TRANSITION RATES OF TRIAXIAL NUCLEI

For a nucleus with axial symmetry, the reduced transition probability $B(E2)$ is related to the intrinsic quadrupole moment Q_0 :

$$B(E2; I_i, K \rightarrow I_f, K) = \frac{5}{16\pi} (eQ_0)^2 \langle I_i K 2 0 | I_f K \rangle^2, \quad (1)$$

where K is the projection of the angular momentum on the symmetry axis. The vector coupling coefficient approaches $\sqrt{3/8}$ in the high-spin limit ($I \gg K$). Obviously this expression cannot be used in the case of a triaxial nucleus. In the case where there is no symmetry axis, it is easier to use the axis of rotation as the quantization axis. Using the quadrupole parameters $Q_0 = \frac{4}{5}ZR^2\beta \cos \gamma$ and $Q_2 = -\frac{4}{5\sqrt{2}}ZR^2\beta \sin \gamma$, the E2 operator quantized along the rotation axis becomes

$$\hat{Q}_\mu = D_{\mu 0}^2 Q_0 + (D_{\mu 2}^2 + D_{\mu -2}^2) Q_2. \quad (2)$$

Assuming the rotation axis to be perpendicular to the axis to which Q_0 and Q_2 are referred, for $\Delta I = 2$ transitions in the high-spin limit one obtains

$$\hat{Q}_2 \approx \sqrt{\frac{3}{8}} Q_0 + \frac{1}{2} Q_2 = \frac{4}{5\sqrt{2}} ZR^2\beta \cos(\gamma + 30^\circ). \quad (3)$$

The reduced transition probabilities within a band with fully aligned spin and the rotation axis as quantization axis can be written using the above definition as

$$B(E2; I, K=I \rightarrow I-2, K=I-2) = \frac{5}{16\pi} (e\hat{Q}_2)^2 \langle I I 2 -2 | I-2 I-2 \rangle^2 = \frac{5}{16\pi} (e\hat{Q}_2)^2 \frac{2I-3}{2I+1}. \quad (4)$$

Note that K is now the projection of the angular momentum on the rotation axis. The wobbling band with $n_w = 0$ has (in a good approximation) fully aligned spin, *i.e.* $K = I$, whereas the $n_w = 1$ band has the collective angular momentum R tilted away from the rotation axis so that $K = I - 1$. For wobbling bands in general it is $K = I - n_w$. Accordingly, for the one-phonon band one can write

$$B(E2; I, K=I-1 \rightarrow I-2, K=I-3) = \frac{5}{16\pi} (e\hat{Q}_2)^2 \langle I I-1 2 -2 | I-2 I-3 \rangle^2 = \frac{5}{16\pi} (e\hat{Q}_2)^2 \frac{(2I-4)(2I-3)}{(2I)(2I+1)}. \quad (5)$$

These expressions allow to extract the expected differences of the in-band $B(E2)$ values for the $n_w = 0$ and $n_w = 1$ bands due to the different coupling schemes. This expected difference changes from 12% at the bottom of the bands to 4% at the highest spins. Around spin 30 where lifetimes could be measured, the expected difference in $B(E2)$ is about 7%.

LIFETIME MEASUREMENT IN ^{163}Lu

Lifetimes of states in the $n_w = 0$ (TSD1) and $n_w = 1$ (TSD2) bands in ^{163}Lu were measured in a Doppler-shift attenuation measurement [13] using Gammasphere at Lawrence Berkeley National Laboratory. High-spin states in ^{163}Lu were populated in the reaction $^{123}\text{Sb}(^{44}\text{Ca}, 4n)$ at a beam energy of 190 MeV. A total of 1.6×10^9 events with fold five or higher were recorded in a three-day experiment. A ^{123}Sb target of 1 mg/cm² was used and the recoils were slowed down and finally stopped in a 12 mg/cm² gold backing. The 102 Compton-suppressed germanium detectors of Gammasphere were grouped in 17 rings covering angles between 17.3° and 162.7°. The level lifetimes were extracted by the analysis of the Doppler-broadened line shapes observed at various angles with respect to the beam direction. The details of the procedure are described in Ref. [13]. Examples of typical line shapes are shown in Fig. 2 together with the results of the fitting procedure. The first two examples show transitions belonging to band TSD1 with $n_w = 0$ which is populated with $\sim 10\%$ of the yrast intensity. Band TSD2 with $n_w = 1$ carries $\sim 3\%$ of the yrast intensity and the statistics for the transitions is accordingly weaker and the spectra show more contaminants (which were included in the fit). Nevertheless, through simultaneous fitting of the entire cascade observed at different angles, consistent results were found. Eight lifetimes of states in TSD1 and seven in TSD2 were determined. The side-feeding quadrupole moments were treated as free parameters, and in some cases it was possible to gate from above, eliminating side-feeding effects. The results are summarized in Table 1. The quoted errors are those derived from the covariance matrix

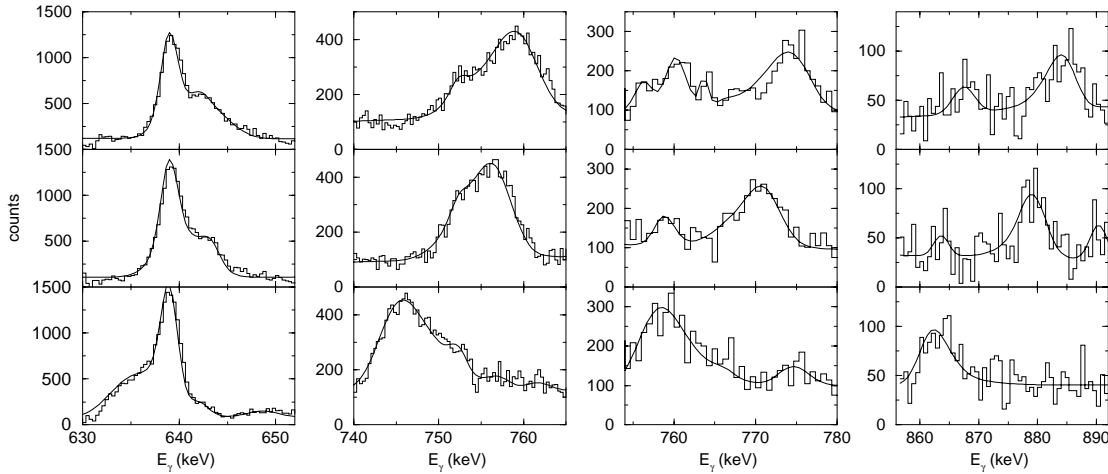


FIGURE 2. Spectra and fitted lineshapes for the (from left to right) 639 and 753 keV transitions of TSD1 and 766 and 873 keV transitions of TSD2, observed at 50° (top), 70° (center), and 130° (bottom). Contaminant peaks are present in some spectra and included in the fit.

TABLE 1. Lifetimes, $B(E2)$ values, and the quadrupole moment as defined in Eq. 2 for the in-band transitions in the $n_w = 0$ band (upper part) and the $n_w = 1$ band (lower part). Note that this quadrupole moment is different from the one generally used for axially symmetric nuclei. The right-hand part shows the absolute $B(E2)$ and $B(M1)$ values for the out-of-band transitions to band TSD1.

I_i^π	E_γ (keV)	τ (ps)	$B(E2)_{in}$ (e^2b^2)	\hat{Q}_2 (b)	E_γ (keV)	$B(E2)_{out}$ (e^2b^2)	$B(M1)_{out}$ (μ_N^2)
41/2 ⁺	578.6	0.364 ^{+0.073} _{-0.085}	3.45 ^{+0.80} _{-0.69}	6.19 ^{+0.72} _{-0.62}			
45/2 ⁺	639.0	0.250 ^{+0.035} _{-0.039}	3.07 ^{+0.48} _{-0.43}	5.81 ^{+0.45} _{-0.41}			
49/2 ⁺	697.0	0.202 ^{+0.021} _{-0.023}	2.45 ^{+0.28} _{-0.25}	5.17 ^{+0.30} _{-0.26}			
53/2 ⁺	752.6	0.119 ^{+0.009} _{-0.010}	2.84 ^{+0.24} _{-0.22}	5.55 ^{+0.23} _{-0.22}			
57/2 ⁺	805.6	0.096 ^{+0.011} _{-0.012}	2.50 ^{+0.32} _{-0.29}	5.20 ^{+0.33} _{-0.30}			
61/2 ⁺	857.7	0.088 ^{+0.010} _{-0.011}	1.99 ^{+0.26} _{-0.23}	4.62 ^{+0.30} _{-0.27}			
65/2 ⁺	909.7	0.067 ^{+0.010} _{-0.015}	1.95 ^{+0.44} _{-0.30}	4.57 ^{+0.52} _{-0.35}			
69/2 ⁺	962.5	0.047 ^{+0.017} _{-0.011}	2.10 ^{+0.80} _{-0.48}	4.73 ^{+0.90} _{-0.54}			
47/2 ⁺	654.6	0.215 ^{+0.037} _{-0.048}	2.56 ^{+0.57} _{-0.44}	5.54 ^{+0.62} _{-0.48}	658.9	0.54 ^{+0.13} _{-0.11}	0.017 ^{+0.006} _{-0.005}
51/2 ⁺	711.2	0.144 ^{+0.017} _{-0.022}	2.67 ^{+0.41} _{-0.33}	5.62 ^{+0.43} _{-0.35}	673.2	0.54 ^{+0.09} _{-0.08}	0.017 ^{+0.005} _{-0.005}
55/2 ⁺	766.2	0.095 ^{+0.013} _{-0.018}	2.81 ^{+0.53} _{-0.41}	5.73 ^{+0.54} _{-0.42}	686.8	0.70 ^{+0.18} _{-0.15}	0.024 ^{+0.008} _{-0.007}
59/2 ⁺	819.9	0.087 ^{+0.026} _{-0.037}	2.19 ^{+0.94} _{-0.65}	5.03 ^{+1.08} _{-0.75}	701.1	0.65 ^{+0.34} _{-0.26}	0.023 ^{+0.013} _{-0.011}
63/2 ⁺	872.9	0.064 ^{+0.013} _{-0.021}	2.25 ^{+0.75} _{-0.48}	5.08 ^{+0.85} _{-0.54}	716.3	0.66 ^{+0.29} _{-0.24}	0.024 ^{+0.012} _{-0.010}
67/2 ⁺	926.5	0.075 ^{+0.017} _{-0.025}	1.60 ^{+0.52} _{-0.37}	4.26 ^{+0.69} _{-0.49}			
71/2 ⁺	980.2	0.056 ^{+0.017} _{-0.029}	1.61 ^{+0.82} _{-0.49}	4.26 ^{+1.09} _{-0.65}			

of the χ^2 minimization and from the spread of the results obtained for different combination of angles. Systematic errors originating from the choice of stopping powers are not included. The values for the 753, 806, and 858 keV transitions agree within errors with an earlier GASP measurement of Schönwaßer *et al.* [11]. They are, however, in disagreement with older Nordball results by Schmitz *et al.* [10]. Given that the level of statistics in the present Gammasphere data is about 35 times higher than of the Nordball data and that many more angles can be used for the analysis, we feel that the weight of evidence is against the results reported by Schmitz *et al.* The new Gammasphere experiment revealed lifetime data for the $n_w = 1$ wobbling band for the first time. The $n_w = 2$ band TSD3 is populated too weakly ($\sim 1.2\%$) in order to extract reliable lifetimes.

While the lifetimes of states in band TSD1 can be directly converted into the in-band $B(E2)$ strengths, the ones measured in TSD2 have to be corrected for the competing interband decay. Since the branching ratios are difficult to

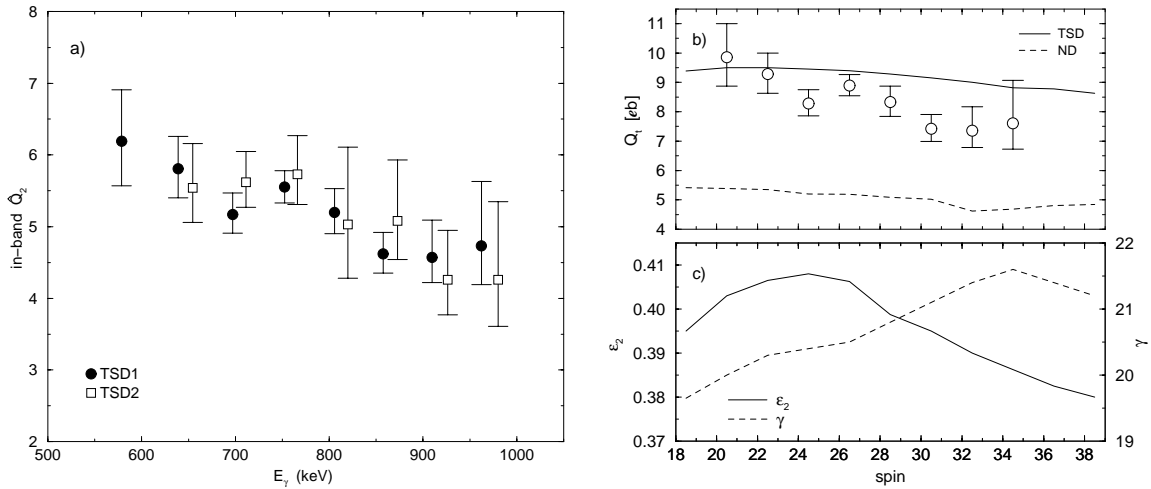


FIGURE 3. a) Quadrupole moments \hat{Q}_2 of the in-band transitions for bands TSD1 and TSD2. b) Comparison of transition quadrupole moments for TSD1 ($Q_t = \sqrt{8/3}\hat{Q}_2$) to values from cranking calculations. c) Quadrupole deformation ϵ_2 (solid line) and triaxiality parameter γ (dashed line) at the triaxial strongly deformed minimum as a function of spin from the cranking calculations.

determine from the Doppler-broadened peaks, the ones measured in a thin-target experiment [9] were used instead. The resulting in-band $B(E2)$ values are presented in Table 1. These can be used to determine the quadrupole moments \hat{Q}_2 with respect to the rotation axis using Eqs. 4 and 5. The results are also found in Table 1 and compared in Fig. 3a). The values for the two bands show a striking similarity as expected for wobbling excitations that are built on the same intrinsic structure. The average ratio $B(E2; n_w = 0)/B(E2; n_w = 1)$ for pairs of transitions with spin I and $I + 1$ is slightly bigger than one, as expected from Eqs. 4 and 5, whereas the in-band quadrupole moments \hat{Q}_2 are almost identical, certainly within the error bars. The similarity of the quadrupole moments cannot stand as a proof for the wobbling scenario alone, but is a necessary condition to be fulfilled by wobbling bands and is, therefore, further evidence for the wobbling motion and stable triaxiality.

Not only do the $B(E2)$ values and quadrupole moments of the two bands show a remarkable similarity, they also exhibit a decrease in the $B(E2)$ and \hat{Q}_2 as the spin increases. The fact that both bands show the same changes further strengthens the argument that they are built on the same intrinsic structure. In order to understand this decrease, the experimental values may be compared to cranking calculations using the ULTIMATE CRANKER code [14]. Since it has been customary for axially symmetric nuclei to refer the quadrupole moments to the symmetry axis, all quadrupole moments have been renormalized by the factor $\sqrt{3/8}$ which is the ratio of \hat{Q}_2/Q_0 in the high-spin limit.

DISCUSSION

The comparison of experimental and calculated transition quadrupole moments (see Fig. 3) show a quite satisfactory agreement, and the calculations reproduce a small decrease in Q_t with spin, although less pronounced than in the experimental data. In the calculation this spin dependence has its origin in the combined effect of a slight decrease in ϵ_2 and an increase in γ from $\sim 19 - 21^\circ$ over the spin range covered by the measurement.

Using the lifetimes of states in band TSD2, the branching ratios from the thin-target data [9], and the mixing ratios from a linear polarization measurement [1], the absolute $B(E2)$ and $B(M1)$ values for the interband decay between bands TSD2 and TSD1 could be established for the first time. The results are shown in the right-hand part of Table 1. Due to the combined uncertainties of the quantities entering, the resulting errors are too large to determine the spin dependence of the interband $B(E2)$ strength, which is expected to be proportional to n_w/I . However, it is possible to use the $B(E2)$ ratios of the interband and in-band transitions for which the uncertainties of the lifetimes do not enter, and compare them to the particle-rotor calculations [7, 8]. The experimental ratio $B(E2)_{out}/B(E2)_{in}$ for the transitions depopulating states in band TSD2 is shown in Fig. 4 as a function of spin together with the results from

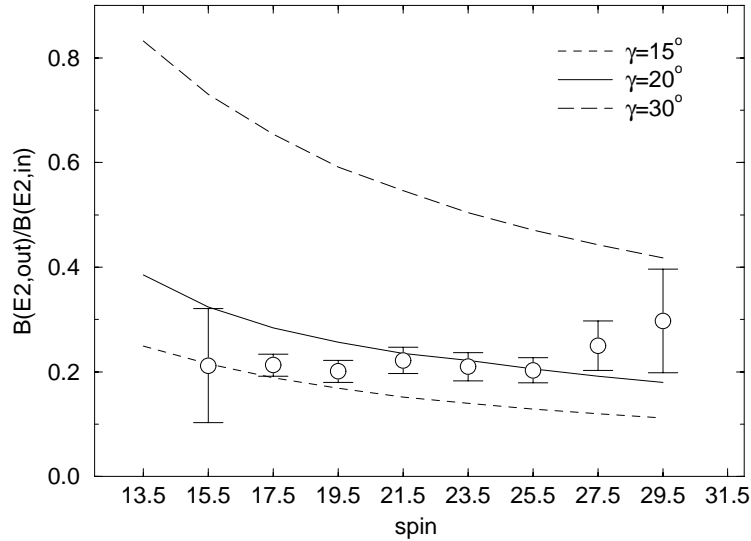


FIGURE 4. Ratio of the interband to in-band $B(E2)$ values for transitions depopulating states of band TSD2 as a function of spin in comparison with particle-rotor calculations for different values of the triaxiality parameter γ .

the particle-rotor calculations. The calculated ratios are shown for different values of the triaxiality parameter γ . Since $B(E2)_{out} \propto \varepsilon_2^2 \sin^2(\gamma + 30^\circ)$ and $B(E2)_{in} \propto \varepsilon_2^2 \cos^2(\gamma + 30^\circ)$, the ratio is independent of the quadrupole deformation ε_2 and exhibits a strong dependence on the triaxiality parameter γ [8]. The experimental $B(E2)$ ratios are constant and do not follow the expected $1/I$ dependence. This behavior could be explained by an increase in triaxiality towards higher spin, which would be in agreement both with the decrease of the in-band $B(E2)$ values and the cranking calculations. An increase from $\gamma \approx 16^\circ$ to $\gamma \approx 22^\circ$ would quantitatively explain the pronounced decrease in the quadrupole moments and, at the same time, explain the constancy of the interband to in-band $B(E2)$ ratios, so that a consistent overall description of the data is reached. The fact that such an increase in γ is stronger than found in the cranking calculations might help to refine the calculations for triaxial nuclei in general.

ACKNOWLEDGMENTS

This research was supported in part by the US DOE under Contract No. DE-AC03-76SF00098, the Danish Science Foundation, and the German BMBF under Contract No. 06 BN 907.

REFERENCES

1. S. W. Ødegård *et al.*, Phys. Rev. Lett. **86**, 5866 (2001).
2. D. R. Jensen *et al.*, Phys. Rev. Lett. **89**, 142503 (2002).
3. G. Schönwaßer *et al.*, Phys. Lett. **B552**, 9 (2003).
4. H. Amro *et al.*, Phys. Lett. **B553**, 197 (2003).
5. P. Bringel *et al.*, to be published.
6. A. Bohr and B. Mottelson, *Nuclear Structure* (Benjamin, New York 1975), Vol. II, pp. 190 ff.
7. I. Hamamoto, Phys. Rev. C **65**, 044305 (2002).
8. I. Hamamoto and G.B. Hagemann, Phys. Rev. C **67**, 014319 (2003).
9. D.R. Jensen *et al.*, Nucl. Phys. **A703**, 3 (2002).
10. W. Schmitz *et al.*, Phys. Lett. **B303**, 230 (1993).
11. G. Schönwaßer *et al.*, Eur. Phys. J. A **13**, 291 (2002).
12. G. Schönwaßer *et al.*, Eur. Phys. J. A **15**, 435 (2002).
13. A. Görge *et al.*, Phys. Rev. C **69**, 031301(R) (2004).
14. T. Bengtsson, Nucl. Phys. **A512**, 124 (1990).